

# 1 **Can land use land cover change explain the reduced resilience** 2 **in forests?**

3 **Sara Alibakhshi**<sup>1\*</sup>, **Hossein Azadi**<sup>2,3,4</sup>, **Leonardo Espinosa-Leal**<sup>5</sup>

4 1 Department of Geosciences and Geography, University of Helsinki, Finland;

5 2 Department of Economics and Rural Development, Gembloux Agro-Bio Tech, University  
6 of Liège, Gembloux, Belgium

7 3 Faculty of Environmental Sciences, Czech University of Life Sciences Prague, Prague,  
8 Czech Republic

9 4 Faculty of Environmental Science and Engineering, Babeş-Bolyai University, Cluj-  
10 Napoca, Romania

11 5 School of Research and Graduate Studies, Arcada University of Applied Sciences,  
12 Helsinki, Finland

13

## 14 **Abstract**

15 Detecting abrupt transitions in ecosystems, known as regime shifts, holds immense  
16 implications for conservation and management endeavors. This research aims to investigate  
17 the feasibility of developing an early warning system capable of identifying an upcoming  
18 critical transition within Mangrove Forest ecosystems. Employing a fusion of remote sensing  
19 analysis, time series analysis, and the critical slowing down theory, Mangrove Forests' state  
20 change was explored across two distinct study sites. One site has been adversely affected by  
21 disturbances stemming from land-use and land-cover changes, while the other serves as an  
22 unaffected reference ecosystem. The study uses data from the Moderate Resolution Imaging  
23 Spectroradiometer (MODIS) satellite, quantifying three remotely sensed indices: the

24 Normalized Difference Vegetation Index (NDVI), the Modified Normalized Difference Water  
25 Index (MNDWI), and the Modified Vegetation Water Ratio (MVWR). Furthermore, temporal  
26 alterations in land-use and land cover are scrutinized using Landsat data from 1996, 2002, 2008,  
27 and 2014. To identify early warning signals of critical transitions, indicators such as  
28 autocorrelation, skewness, and standard deviation are applied. The results show the robust  
29 capabilities of remote sensing in generating early warning signals of critical transition in  
30 Mangrove Forests. NDVI outperformed MVWR and MNDWI as ecosystem state indicators.  
31 This study not only highlights the potential of remote in identifying the approaching regime  
32 shifts in Mangrove Forest ecosystems but also adds knowledge on ecosystem dynamics. This  
33 is the first report of the successful application of remote sensing in generating early warning  
34 signals for imminent critical transitions within Mangrove forests in the Middle East.

35

36 **Keywords:** land-use and land cover-change, monitoring ecosystem dynamics, remote sensing,  
37 Mangrove Forests.

## 38 **1. Introduction**

39 Mangrove forests play a crucial role in providing valuable ecosystem services, contributing to  
40 a staggering annual value of at least US \$1.6 billion (Polidoro, Carpenter et al. 2010). These  
41 services encompass a wide range of benefits that support coastal livelihoods on a global scale  
42 (Dahdouh-Guebas, Jayatissa et al. 2005, Duke, Meynecke et al. 2007, Ellison 2008, Abrantes,  
43 Johnston et al. 2015). However, Mangrove forests are disappearing worldwide by 1 to 2% per  
44 year (Duke, Meynecke et al. 2007). Clearing for coastal development, expansion of aquaculture,  
45 logging for timber, and fuel production are among the primary drivers behind this concerning  
46 trend (Daru, Yessoufou et al. 2013, Kirui, Kairo et al. 2013, Yessoufou and Stoffberg 2016). It  
47 has been shown that over 40% of the assessed vertebrate species endemic to Mangrove Forests  
48 are currently facing global threats to their survival (Luther and Greenberg 2009). As a result,  
49 urgent attention is needed to monitor the state of Mangrove forests and get a better  
50 understanding of Mangrove Forest dynamics in response to disturbances.

51  
52 The response of an ecosystem, such as the Mangrove ecosystem, to disturbance is not always  
53 a gradual process; it can lead to sudden and irreversible changes (Scheffer 1990, Scheffer 2001,  
54 Scheffer, Carpenter et al. 2001). In fact, even gradual changes in the environment may not  
55 result in a corresponding gradual response from the ecosystem. Instead, they can trigger sudden,  
56 unpredictable, and irreversible shifts known as regime shifts (Capon, Lynch et al. 2015). Apart  
57 from the growing evidence of critical changes occurrences in different ecosystems (Barbier,  
58 Koch et al. 2008, Guttal and Jayaprakash 2008, Lenton 2011, Verbesselt, Umlauf et al. 2016,  
59 Alibakhshi, Groen et al. 2017), the need to enhance the understanding of generating early  
60 warning signals of critical transition in ecosystems is highlighted.

61  
62 Abrupt changes in the state of an ecosystem can occur when ecosystems are unable to cope  
63 with the effects of disturbances, leading to slower resilience and a reduced ability to recover  
64 (Carpenter and Brock 2006, Carpenter, Brock et al. 2008, Scheffer, Bascompte et al. 2009,

65 Carpenter and Brock 2011, Carpenter, Cole et al. 2011). Disturbances can push the state of an  
66 ecosystem to a state that is near a critical threshold. Once a critical threshold is reached, even  
67 a small disturbance can trigger a significant transition to a new state, where it is challenging  
68 and sometimes impossible to return to the previous state (Scheffer, Carpenter et al. 2001,  
69 Carpenter and Brock 2006, Carpenter, Brock et al. 2008, Scheffer, Bascompte et al. 2009,  
70 Carpenter and Brock 2011, Carpenter, Cole et al. 2011). This knowledge is crucial for assessing  
71 the current state of an ecosystem and determining whether it is approaching a critical transition.  
72 Understanding the current state of an ecosystem is particularly crucial in Mangrove Forests, as  
73 it can inform conservation efforts and has abundant resources and socio-economic impacts for  
74 locals (Martínez, Intralawan et al. 2007). Detecting the state of an ecosystem can prevent  
75 irreversible changes and facilitate early interventions (Lenton, Held et al. 2008, Hirota,  
76 Holmgren et al. 2011, Alibakhshi 2023).

77

78 Various methods have been developed to quantify the state of an ecosystem (Carpenter and  
79 Brock 2006, Dakos, Carpenter et al. 2012, Kéfi, Guttal et al. 2014). For example, an increasing  
80 trend in autocorrelation and standard deviation of the state variables over time (Dakos, Van Nes  
81 et al. 2012) can serve as reliable early warning signals, indicating an approaching critical  
82 transition in the ecosystem (Dakos, Carpenter et al. 2012, Dakos, Van Nes et al. 2012, Lenton,  
83 Livina et al. 2012, Dakos, Carpenter et al. 2015). Furthermore, disruptions or disturbances  
84 within the ecosystem can lead to alterations in the asymmetrical distribution of the state  
85 variable time series, resulting in an increased skewness, which can be served as early warning  
86 signals of critical transition (Guttal and Jayaprakash 2008, Dakos, Carpenter et al. 2012).

87

88 Despite the availability of various methods for assessing early warning signals (Eslami-  
89 Andergoli, Dale et al. 2015), the anticipation of critical transitions in ecosystems poses  
90 significant challenges. Hence, the application of the methods to assess the state of ecosystems  
91 and identify early warning signals of critical transition in the state of ecosystems is still limited.  
92 The complexity and diversity of ecological systems, coupled with the need for high-frequency

93 observations and comprehensive time series data on relevant environmental variables, present  
94 significant obstacles (Dakos, Carpenter et al. 2015). To address this problem, this study is using  
95 the high spatio-temporal resolution of satellite images. Satellite images offer high-resolution,  
96 comprehensive coverage, and multispectral capabilities, making them a powerful tool for the  
97 aim of this study.

98

99 To effectively detect the approach of an ecosystem towards a critical threshold, it is crucial to  
100 select the right state variables, which is variable that can accurately present the state of an  
101 ecosystem and measure the proximity of the ecosystem to critical conditions (Alibakhshi,  
102 Groen et al. 2017). For example, a research study has demonstrated that the utilization of  
103 remotely sensed indicators capable of simultaneously capturing variations in both water and  
104 vegetation can provide a more comprehensive understanding of the state of an ecosystem  
105 compared to relying solely on vegetation-based or water-based indices (Alibakhshi, Groen et  
106 al. 2017).

107

108 This study aims to investigate the potential of time series analysis of remote sensing data in  
109 detecting regime shifts in Mangrove Forest ecosystems and establishing an early warning  
110 system. As two main components of Mangrove Forests are vegetation and water, a vegetation-  
111 based indicator, namely the Normalized Difference Vegetation Index (NDVI), a water-based  
112 indicator, namely the Modified Normalized Difference Water Index (MNDW), and a  
113 vegetation-water-based indicator, namely Modified Vegetation Water Ratio (MVWR) has been  
114 employed as remotely sensed state variables. Additionally, changes in land-use and land cover-  
115 change are quantified using Landsat data from 1996, 2002, 2008, and 2014 to assess the reasons  
116 behind the reduced resilience and possible early warning signals of upcoming critical transition  
117 in study sites. Mangrove Forest ecosystems in Qeshm Island and Gabrik are chosen as case  
118 studies, where Qeshm Island is selected as a representative of an unhealthy ecosystem, while  
119 Gabrik serves as the reference site for comparison. The application of critical slowing down in  
120 monitoring Mangrove Forests has been rarely tested (Wang, Zhang et al. 2023). This is the first

121 study that explores the potential of remote sensing to explore early warning signals of  
122 impending critical transition in Mangrove forests in Iran.

## 123 **2. Material and Methods**

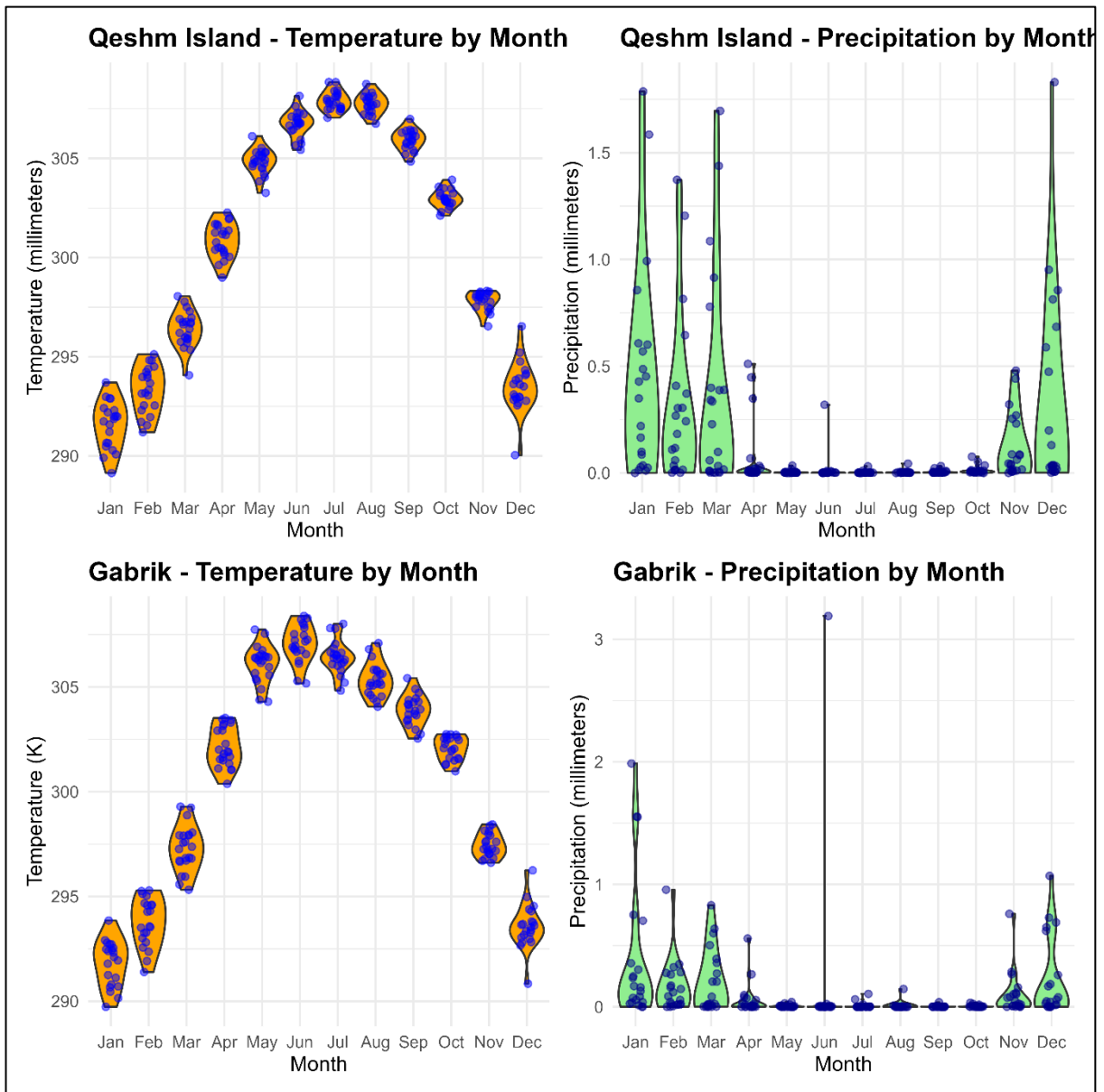
### 124 **2.1. Study Area**

125

126 This study focuses on Qeshm Island (Mazraeh and Pazhouhanfar 2018, Kourosh Niya, Huang  
127 et al. 2019), located in the southern region of Iran, between the Persian Gulf and the Oman Sea.  
128 Qeshm Island, with a total area of 1667 km<sup>2</sup>, has undergone substantial and, at times, drastic  
129 changes in its land-use and land cover-change time (Kourosh Niya, Huang et al. 2019). Gabrik,  
130 with a total area of 2496 km<sup>2</sup>, has been selected as a reference case study, representing a healthy  
131 ecosystem. Gabrik shares identical climatic conditions with Qeshm Island and is also  
132 characterized by the presence of Mangrove Forest ecosystems (Zahed, Rouhani et al. 2010,  
133 Naderloo, Türkay et al. 2013).

134

135 The geographical coordinates of Qeshm Island range from 55° 15' 38" to 56° 16' 52" E and 26°  
136 32' 20" to 27° 00' 00" N, and Gabrik is located southeast of Qeshm Island with geographical  
137 coordinates ranging from 55° 15' 38" to 56° 16' 52" E and 26° 32' 20" to 27° 00' 00" N (Fig.  
138 1). Based on ERA5 data (Muñoz Sabater 2019), the mean temperature in Qeshm Island is 301  
139 Kelvin (28 degrees Celsius), and the mean precipitation is 36 mm from February 18, 2000 to  
140 July 31, 2021. In Gabrik, the mean temperature is 301 Kelvin (28 degrees Celsius), with an  
141 average precipitation of 28 mm from February 18, 2000 to July 31, 2021. These show the  
142 similarity of climatic conditions and local weather patterns of Qeshm Island and Gabrik study  
143 sites (Fig. 1). According to the population dataset provided by WorldPop (Sorichetta, Hornby  
144 et al. 2015), the estimated population residing in the region of Gabrik is reported to be  
145 remarkably low, with a mere 74 individuals. On the other hand, a significantly higher  
146 population count of 957 individuals are living in Qeshm Island.



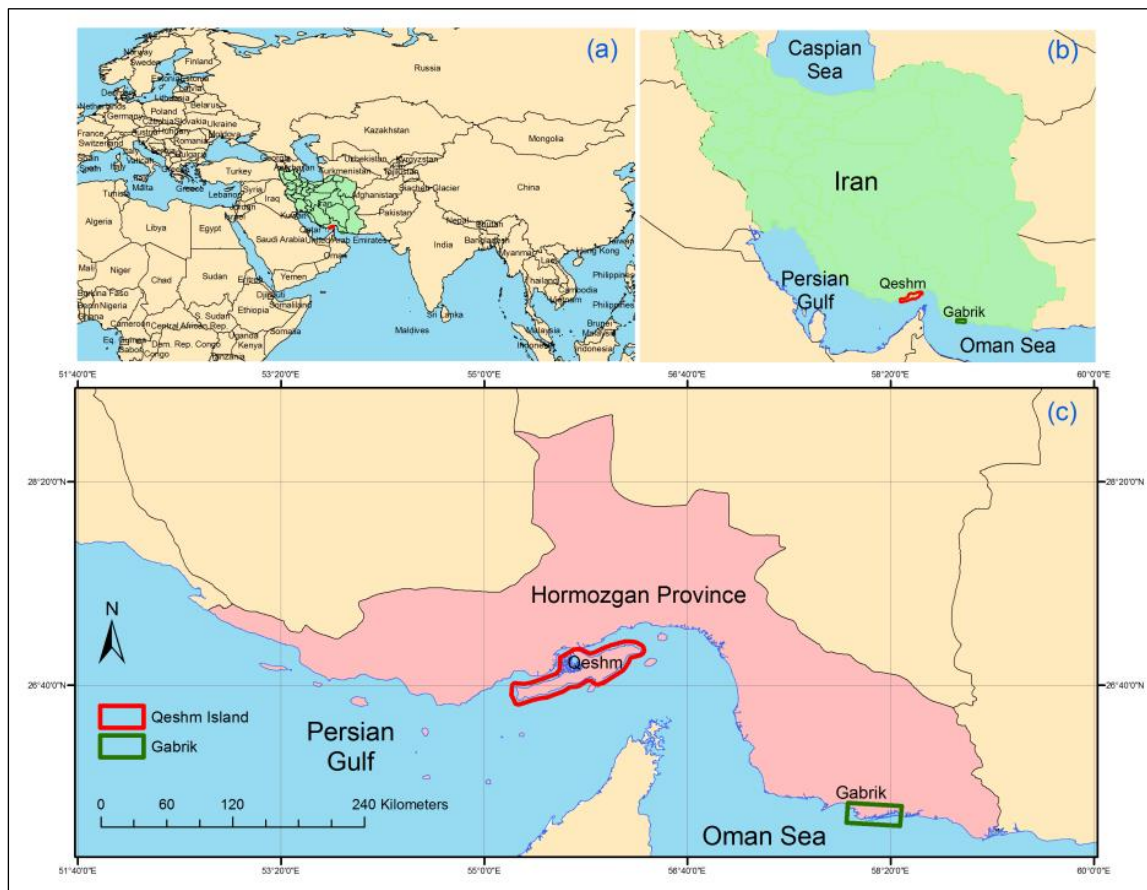
147

148

Figure 1. Monthly temperature in Kelvin ( $^{\circ}\text{K}$ ) and precipitation millimetres (mm) for Qeshm

149

Island and Gabrik from February 18, 2000, to July 31, 2021.



150

151 Figure 2. Location of the study sites Qeshm Island and Gabrik (a:c).

152

## 153 2.2. Materials and data collection

### 154 2.2.1. State variables

155 The Normalized Difference Vegetation Index has been obtained from the latest version of the  
 156 Moderate Resolution Imaging Spectroradiometer (MODIS) product, specifically MOD09A1  
 157 (version 006). The 006 version of MOD09A1 has undergone algorithm enhancements aimed  
 158 at improving its accuracy (Didan, 2015). The data utilized in this study was acquired from the  
 159 Google Earth Engine platform (Gorelick et al., 2017), which offers a comprehensive repository  
 160 of geospatial data. The dataset utilized herein possesses a spatial resolution of 500 meters with  
 161 a temporal resolution of 16 days, enabling comprehensive analysis from February 18, 2000, to  
 162 July 31, 2021. The MOD09A1 product is derived from atmospherically corrected bi-directional  
 163 surface reflectance. The Red and Near-Infrared (NIR) bands, specifically within the

164 wavelengths of 0.620  $\mu\text{m}$  to 0.670  $\mu\text{m}$  and 0.841  $\mu\text{m}$  to 0.876  $\mu\text{m}$ , respectively has been used  
165 to calculate NDVI (Eq. 1). The NDVI values range from -1 to +1, where a value of -1 indicates  
166 bare land, while a value of +1 indicates dense forest.

167

$$\text{NDVI} = \left( \frac{\text{NIR} - \text{Red}}{\text{NIR} + \text{Red}} \right) \quad (\text{Eq. 1})$$

168

169 Furthermore, the Modified Normalized Difference Water Index (MNDWI) is a useful indicator  
170 for identifying and quantifying water bodies within an ecosystem (Xu 2006). MNDWI is  
171 calculated using MOD09A1 (version 006), which is described earlier. Among the numerous  
172 remotely sensed water indices available (Mozumder, Tripathi et al. 2014, Rokni, Ahmad et al.  
173 2014, Li, Chen et al. 2015), MNDWI has been recognized as the most accurate indicator for  
174 extracting water area variations (Ji, Zhang et al. 2009, Chen, Huang et al. 2013). MNDWI,  
175 similar to NDVI, is a dimensionless index that ranges from -1 to 1. When MNDWI values are  
176 below 0, it indicates low water content, which includes soil and vegetation. On the other hand,  
177 MNDWI values above 0 indicate high water content and varying water levels. The Green and  
178 shortwave infrared (SWIR) bands, specifically within the wavelengths of 1.23  $\mu\text{m}$  to 1.25  $\mu\text{m}$   
179 and 0.55  $\mu\text{m}$  to 0.57  $\mu\text{m}$ , respectively has been used to calculate MNDWI (Eq. 2).

$$\text{MNDWI} = \left( \frac{\text{Green} - \text{SWIR}}{\text{Green} + \text{SWIR}} \right) \quad (\text{Eq. 2})$$

180 Additionally, the Modified Vegetation Water Ratio (MVWR) was used to measure early  
181 warning signs in aquatic ecosystems (Alibakhshi, Groen et al. 2017) (Eq. 3). The MVWR is  
182 sensitive to changes in vegetation water content, which are the main component of Mangrove  
183 Forests. It effectively captures variations in water availability and reflects hydrological  
184 dynamics, such as seasonal fluctuations and long-term shifts. Moreover, the MVWR proves  
185 valuable in assessing vegetation health and stress levels (Tehrani and Janalipour 2021).

$$\text{MVWR} = \ln \left( \frac{\text{NDVI} + 1}{\text{MNDWI} + 1} \right) \quad (\text{Eq. 3})$$

186        **2.2.2. Map of mangrove Forest ecosystems and land-use and land cover-change**

187        The land-use and land cover-changes map was calculated with a spatial resolution of 30 meters  
188        (Kouros Niya, Huang et al. 2019), by using Landsat satellite imagery for the years 1996, 2002,  
189        2008, and 2014. The maps provide a classification map of study sites, including six distinct  
190        land use classes: agriculture, bare-land, built-up, dense-vegetation, mangrove (Mangrove  
191        Forest ecosystem), and waterbody.

192

193        In addition, the Global Mangrove Forest Distribution dataset was employed for the year 2000  
194        which provides a map of the world's Mangrove Forest ecosystems as of the year 2000 with a  
195        spatial resolution of approximately 30 meters (Giri, Ochieng et al. 2011, Giri, Ochieng et al.  
196        2013). The data compilation involved analyzing over 1,000 Landsat Thematic Mapper (TM)  
197        scenes using a hybrid approach of classification techniques.

198        **2.3. Methods for exploring early warning signals of critical transition**

199        In this study, we only used a large variety of freely available remotely sensed data. All  
200        statistical analyses and visualizations were performed in R statistical software (Pinheiro, Bates  
201        et al. 2000) QGIS (Qgis 2016), and Google Earth Engine (Gorelick, Hancher et al. 2017).

202

203        First Mangrove Forest ecosystems in each study site were delineated using the Global  
204        Mangrove Forest Distribution maps (Section 2.2.2). Second, 100 points in each study site were  
205        randomly selected. From each point, the time series of the state variables (Section 2.2.1) was  
206        extracted using a mean function for the period from February 18, 2000, to July 31, 2021. Finally,  
207        autocorrelation, skewness, and standard deviation were applied to detect early warning signals  
208        of critical transition (Dakos, Carpenter et al. 2012). More specifically, autocorrelation refers to  
209        the degree of correlation between the values of the same variables in different observations in  
210        the data. The concept of autocorrelation is usually used in time series data to calculate the  
211        correlation of value to itself in different observations over a consecutive time. For  
212        autocorrelation calculation, the first step is to define a lag operator, which is represented by ( $t$ )

213 and is a time display. The autocorrelation function (ACF) can be calculated using equation (4):

$$ACF = \frac{\sum_{i=1}^n (x_i - \mu)(x_{i-t} - \mu)}{\sum_{i=1}^n (x_i - \mu)^2} \quad (\text{Eq. 4})$$

214 Standard deviation (SD) measures the degree of variability or distribution for a set of data  
215 relative to the mean of the same data. SD is obtained from the variance as shown in equation  
216 (5):

$$SD = \sqrt{\frac{1}{n-1} \sum_{t=1}^n (x_t - \mu)^2} \quad (\text{Eq. 5})$$

217 Skewness is the third statistical index used in this study, which is calculated using equation (6):

$$SK = \frac{\frac{1}{n} \sum_{t=1}^n (x_t - \mu)^3}{\sqrt{\frac{1}{n} \sum_{t=1}^n (x_t - \mu)^2}} \quad (\text{Eq. 6})$$

218 Prior to applying metric-based models, the data needs to undergo detrending and smoothing  
219 procedures to mitigate the impact of nonstationary conditions on the leading indicators (Dakos,  
220 Carpenter et al. 2012). Several detrending approaches are commonly employed, such as  
221 Gaussian, Linear, Loess filters, and first-differencing (Lenton, Livina et al. 2012). These  
222 methods detrend the data within a rolling window. In this study, a sensitivity analysis was  
223 conducted using Kendall's  $\tau$ , a nonparametric statistic measuring the association between  
224 indicators and time, to identify the optimal size of the rolling window and bandwidth for the  
225 Gaussian filter (Bevan and Kendall 1971). Kendall's  $\tau$  ranges from -1 to +1, where higher  
226 values indicate stronger trends, aiming to identify the detrending settings that best capture  
227 trends in the leading indicators. To achieve this, the leading indicators for various rolling  
228 window sizes (ranging from 25% to 75% of the time series length) and bandwidths (ranging  
229 from 25% to 75% of the time series length for the Gaussian filter) with increments of 10%,  
230 using Gaussian, Loess, Linear filters, and first-differencing approaches was calculated.

231

232 To ensure that the observed trends in the leading indicators were not due to random chance,  
233 1000 surrogate datasets were generated. These datasets were created by fitting the best linear  
234 autoregressive moving average model (ARMA) based on AIC to the residuals obtained after

235 detrending the data. Each surrogate dataset had the same length as the residual time series.  
236 Following previous research, the trend estimations from the original data with those from the  
237 surrogate data, had similar correlation structures and probability distributions. Kendall's  $\tau$  was  
238 employed to estimate trends in autocorrelation, skewness, and standard deviation was  
239 compared. The probability of finding a trend by chance was measured by comparing Kendall's  
240  $\tau$  of the original data with the number of cases in which the statistic was equal to or smaller  
241 than the estimates of the simulated records, denoted as  $P(\tau^* \leq \tau)$  (Dakos, Carpenter et al.  
242 2012). Additionally, when a clear breakpoint was present in the time series, Kendall's  $\tau$  for the  
243 period before the breakpoint was reported to ensure robust trend estimations.

## 244 **3. Results**

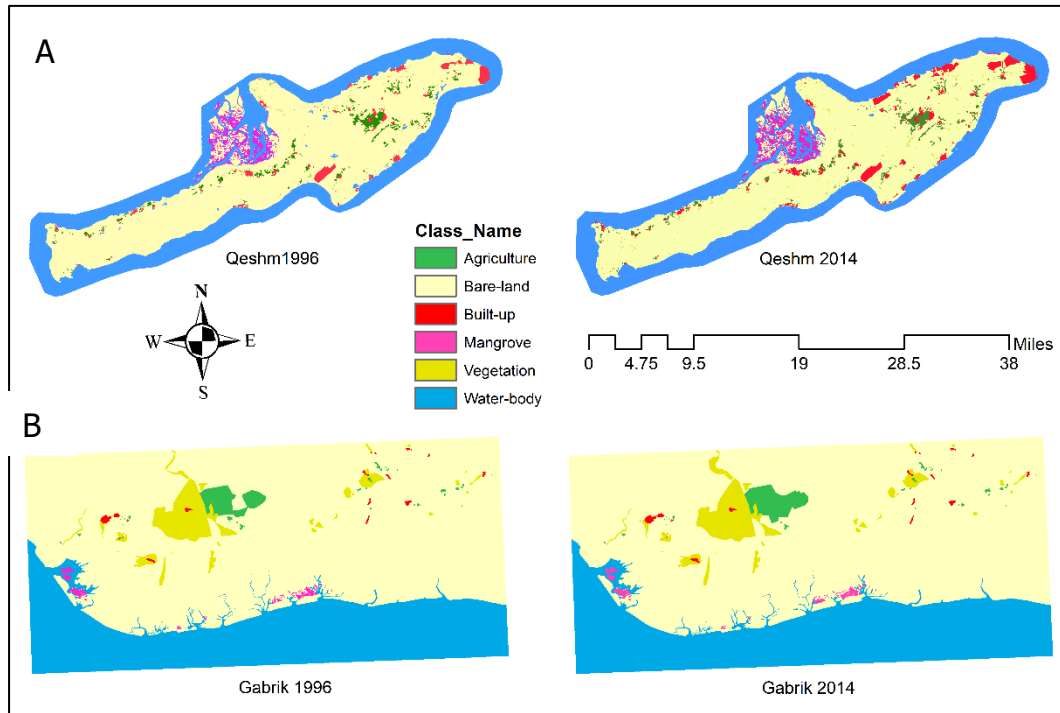
245 The Results include an analysis of land-use and land cover-change in Qeshm Island and Gabrik,  
246 highlighting changes in agriculture, bare land, built-up areas, mangroves, vegetation, and water  
247 bodies (Section 3.1). Time series of state variables, including NDVI, MNDWI, and MVWR  
248 are represented, which show temporal dynamics and seasonal variations of Mangrove Forests  
249 in study sites (Section 3.2). Finally, the early warning signals observed time series of NDVI,  
250 MNDWI, and MVWR have been presented (Section 3.3).

### 251 **3.1. land-use and land cover-change**

252 Qeshm Island experienced various changes in land-use and land cover-change during the study  
253 period (Table. 1). The area dedicated to agriculture witnessed a marginal increase of 338 units  
254 (0.65% change). However, there was a significant decrease in bare land, with a change of -  
255 57,360 units (-3.65% change). On the other hand, built-up areas expanded dramatically,  
256 showing an increase of 35,759 units (64.40% change). Mangroves and vegetation also  
257 exhibited positive growth, with changes of 6,049 units (9.07% change) and 6,880 units (70.30%  
258 change), respectively. Water bodies slightly expanded, with a change of 8,336 units (0.82%  
259 change).

260

261 In Gabrik agriculture experienced substantial growth (Table. 1), with a change of 4,708 units  
262 (15.22% change). Bare land decreased, albeit to a lesser extent, with a change of -8,629 units  
263 (-0.52% change). The built-up areas expanded modestly, with a change of 215 units (4.04%  
264 change). Mangroves and vegetation also showed positive growth, with changes of 790 units  
265 (9.47% change) and 2,628 units (3.22% change), respectively. Water bodies remained relatively  
266 stable, with a minimal change of 288 units (0.04% change).



267  
268 Figure 3. Land-use maps of Qeshm Island (A) and Gabrik (B) were extracted from Landsat  
269 images from 1996 to 2014.  
270

271 Table 1. land-use and land cover-change in Qeshm Island and Gabrik between 1996 and 2014,  
 272 obtained from Landsat data at 30-m spatial resolution.

Case study	Class	1996 (number of pixels)	2014 (number of pixels)	Change (number of pixels)	Percentage (%)
Qeshm	Agriculture	51615	51953	338	0.65%
	Bare-land	1571765	1514405	-57360	-3.65%
	Built-up	55525	91284	35759	64.40%
	Mangrove	66672	73552	6049	9.07%
	Vegetation	9787	15836	6880	70.30%
	Water-body	1012778	1021114	8336	0.82%
Gabrik	Agriculture	30929	35637	4708	15.22%
	Bare-land	1674507	1665878	-8629	-0.52%
	Built-up	5317	5532	215	4.04%
	Mangrove	8342	9132	790	9.47%
	Vegetation	81579	84207	2628	3.22%
	Water-body	657401	657689	288	0.04%

273

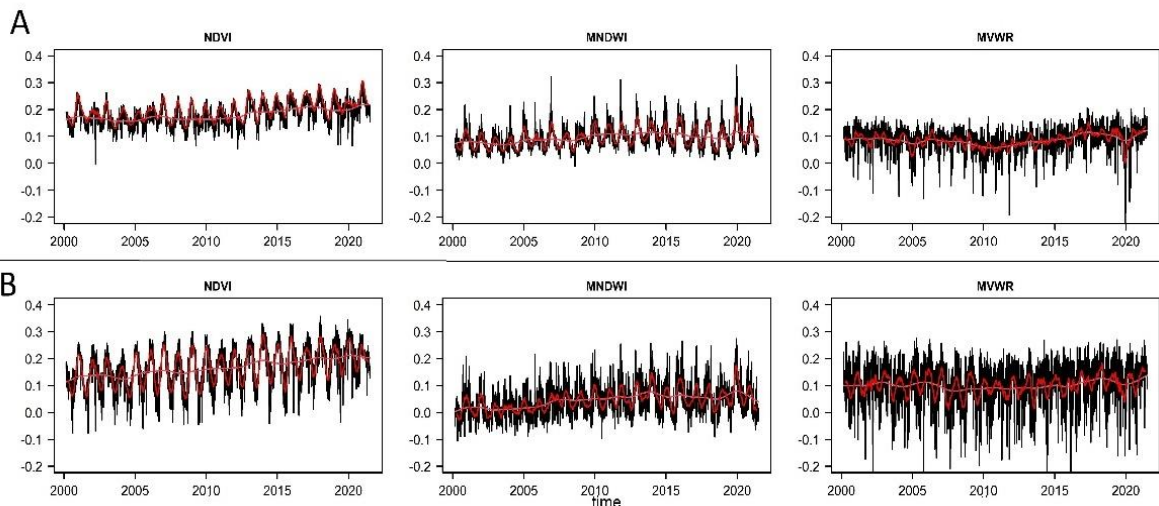
### 274 3.2. Time series of state variables

275 The extracted data for the NDVI, MNDVI, and MVWR indices represent temporal dynamics  
 276 and seasonal variations in study sites (Fig. 5). The data presented in the table consists of four  
 277 variables: time, NDVI, MNDWI, and MVWR. The time column represents the date of the  
 278 measurements. The NDVI values range from 0.01 to 0.36, indicating the density of green  
 279 vegetation cover in the study area. The MNDWI values range from -0.01 to 0.36, representing  
 280 the presence of water bodies. The MVWR values range from -0.242 to 0.263, indicating the  
 281 vegetation's water content. In Gabrik, the NDVI values range from -0.078 to 0.35, indicating  
 282 the density of green vegetation cover in the study area. The MNDWI values range from -0.10  
 283 to 0.27, representing the presence of water bodies. The MVWR values range from -0.25 to 0.27,

284 indicating the vegetation's water content.

285

286 Qeshm Island has a slightly higher average NDVI value of 0.20, indicating a relatively denser  
287 green vegetation cover compared to Gabrik, which has an average NDVI of 0.17. This suggests  
288 that Qeshm Island may have a higher overall vegetation density. In terms of water presence,  
289 Gabrik exhibits a lower average MNDWI value of 0.04, suggesting a relatively lower presence  
290 of water bodies compared to Qeshm Island, which has an average MNDWI of 0.10. This  
291 indicates that Qeshm Island may have more abundant water bodies within its study area.  
292 Regarding vegetation water content, Gabrik and Qeshm Island have similar average MVWR  
293 values of 0.10 and 0.09, respectively.



294

295 Figure 4. The time series of three remotely sensed indices. The first column represents time  
296 series of Normalized Difference Vegetation Index (NDVI), the second column represents  
297 Modified Normalized Water Index (MNDWI), and the third column represents Modified  
298 Vegetation Water Ratio (MVWR) from February 18, 2000, to July 31, 2021, at 500-m spatial  
299 resolution in Qeshm Island (A) and Gabrik (B). The red line illustrates the trend obtained using  
300 a moving average with a window size of 20-time steps.

301

### 302 3.3. Early warning signals of a critical transition

303 Comparing the values obtained for autocorrelation, Qeshm exhibited significantly higher

304 values (0.411, 0.817, and 0.181) compared to Gabrik (0.037, -0.046, and 0.004), indicating a  
 305 stronger temporal dependency within the ecosystem. Conversely, Gabrik displayed relatively  
 306 lower autocorrelation values. Furthermore, the analysis of standard deviation demonstrated  
 307 notably higher values for Qeshm (0.535, 0.827, and -0.207) compared to Gabrik (-0.689, 0.652,  
 308 and -0.483). Regarding skewness, Qeshm exhibited positive values (0.631, 0.401), while  
 309 Gabrik displayed negative values (-0.199, -0.191) for NDVI and MNDWI indices. These  
 310 contrasting skewness values indicate asymmetry in the distribution of the variables.

311

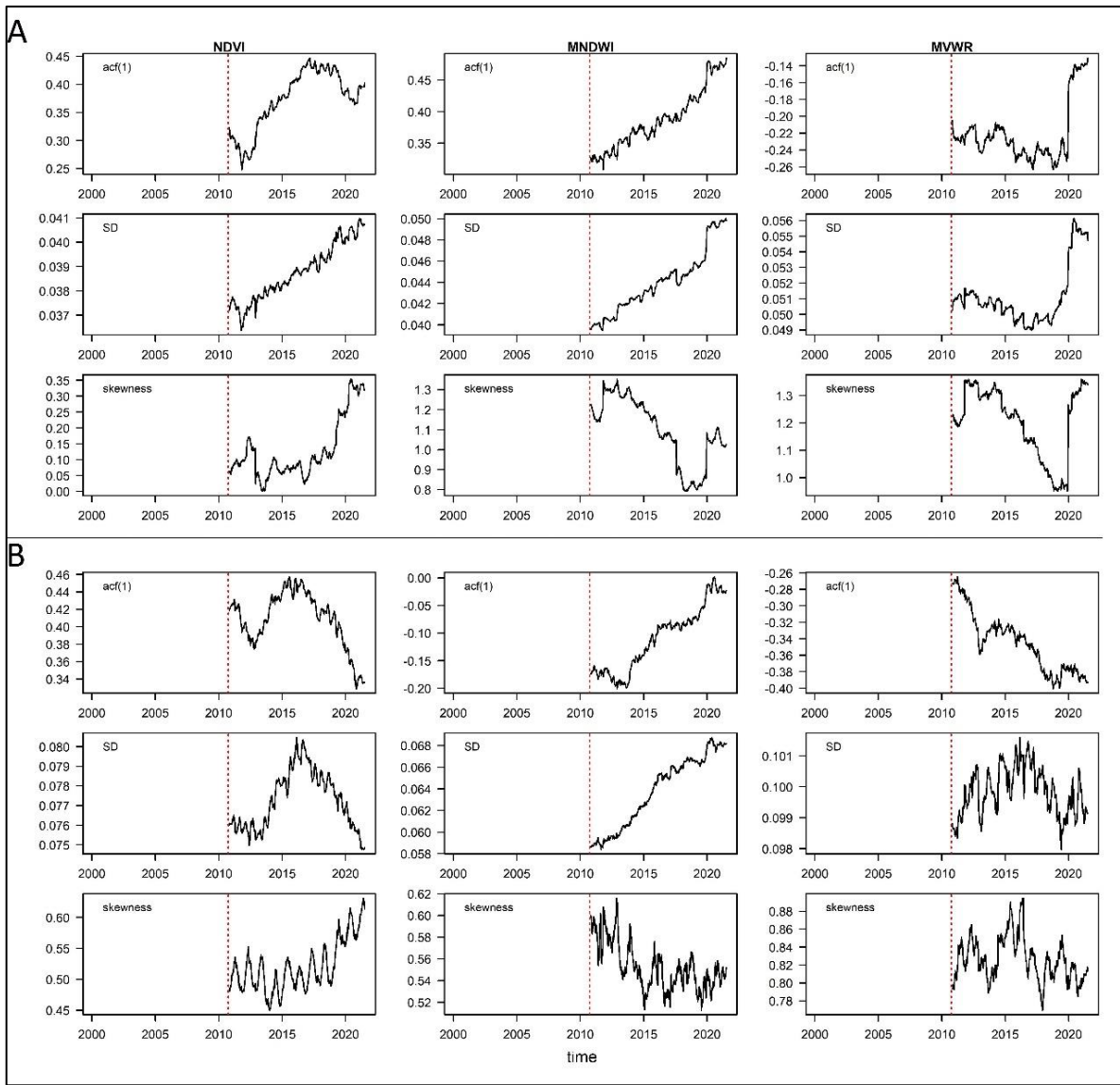
312 Table 2. Kendall's  $\tau$  trend of autocorrelation, standard deviation, and skewness in Qeshm Island  
 313 and Gabrik (significant at  $P < 0.1$ ) of Normalized Difference Vegetation Index (NDVI),  
 314 Modified Normalized Water Index (MNDWI), and Modified Vegetation Water Ratio (MVWR)  
 315 from February 18, 2000, to July 31, 2021.

Statistical Measures	Qeshm			Gabrik		
	NDVI	MNDWI	MVWR	NDVI	MNDWI	MVWR
Autocorrelation	0.411	0.817	0.181	0.037	-0.046	0.004
Standard Deviation	0.535	0.827	-0.207	-0.689	0.652	-0.483
Skewness	0.631	0.401	-0.271	-0.199	-0.191	0.07

316

317

318



319

320 Figure 5. Early warning signals analysis using time series of remotely sensed indices. The first  
 321 column represents Normalized Difference Vegetation Index (NDVI), the second column  
 322 represents Modified Normalized Water Index (MNDWI), and third column represents  
 323 Modified Vegetation Water Ratio (MVWR) from February 18, 2000, to July 31, 2021, at 500-  
 324 m spatial resolution in Qeshm Island (A), and Gabrik (B). The red line illustrates the rolling  
 325 window size of 50 percent which was used in the analysis. The acf(1) refers to autocorrelation  
 326 at lag one, SD refers to standard deviation.

327

## 4. Discussion

This study illuminates the provision of early warning signals for abrupt changes in the Mangrove Forest ecosystem, offering valuable information about the impact of land-use and land cover-change on ecosystem dynamics. Mangrove Forest ecosystems are crucial for biodiversity conservation, harboring a diverse range of plant and animal species and providing vital habitats and breeding grounds for numerous marine and avian organisms, contributing to the overall ecological resilience of coastal ecosystems (Nagelkerken, Van der Velde et al. 2000, Lugendo, Nagelkerken et al. 2007, Kathiresan 2012). The results showed although the study sites, Qeshm Island and Gabrik share similar climate, geography, and annual rainfall (Fig.1, Fig. 2), the analysis of remote sensing indices, including NDVI, MNDWI, and MVWR, revealed notable differences between the two study areas (Fig. 4). Comparing Qeshm Island and Gabrik, it is evident that the expansion of built-up areas was more prominent in Qeshm Island than in Gabrik (Table. 1) which can explain the differences in the remotely sensed indices that are representing the variations in vegetation and water (Fig. 4) and observed early warning signals (Fig. 5) in Mangrove Forest ecosystems.

The results revealed that in Qeshm Island, autocorrelation has increased in all three indices compared to Gabrik (Fig. 5), indicating early warning signals of upcoming critical transition and also loss of resilience in coping with the stress of disturbances. In addition, Qeshm Island exhibited higher standard deviation and skewness values, than Gabrik, indicating greater variability and asymmetry in the distribution of index values. These findings suggest that Qeshm Island experiences more pronounced fluctuations which presents a high potential for ecosystem state change occurrences compared to Gabrik (Fig. 5). The observed early warnings could be attributed to various factors such as land-use and land cover-change in the area (Table 1.). The expansion of built-up areas in Qeshm Island, as evidenced by the significant increase in urban development, raises concerns about its potential impacts on the island's ecological balance (Fig. 3 and Table 2). Previous studies also have shown that Qeshm Island has

356 undergone a lot of changes, from land-use and land cover-change (Toosi, Soffianian et al. 2019,  
357 Tajbakhsh, Karimi et al. 2020), to petroleum pollution (Ebrahimi-Sirizi and Riyahi-Bakhtiyari  
358 2013). In contrast, Gabrik, being the reference site, showed relatively lower values for  
359 autocorrelation, standard deviation, and skewness. This indicates a more stable and consistent  
360 pattern of index values, implying a healthier and less perturbed ecosystem compared to Qeshm  
361 Island (Figs 4 and 5). The lower variability and symmetry in the distribution of data imply a  
362 more balanced and stable state in terms of land cover and ecological conditions (Guttal and  
363 Jayaprakash 2008).

364

365 The results showed that NDVI outperformed MVWR and MNDWI as a robust indicator of  
366 ecosystem dynamics for several reasons (Fig.5). The NDVI, which provides information about  
367 vegetation cover (Alatorre, Sánchez-Carrillo et al. 2016, Li, Jia et al. 2019, Alibakhshi 2020,  
368 Cabello, Germentil et al. 2021), proved to be highly sensitive in capturing changes in Mangrove  
369 Forest ecosystems. The NDVI has been widely used and validated in numerous studies for  
370 assessing vegetation dynamics (Verbesselt, Hyndman et al. 2010, Verbesselt, Hyndman et al.  
371 2010, Ruan, Yan et al. 2022, Tran, Reef et al. 2022). It is based on the principle that healthy  
372 vegetation, such as Mangrove Forest, reflects more near-infrared (NIR) radiation and absorbs  
373 more red light (Eq. 1), resulting in higher NDVI values (Shimu, Aktar et al. 2019). The time  
374 series of NDVI has explained 62 % of the global mangrove loss due to land-use and land cover-  
375 change (Goldberg, Lagomasino et al. 2020). In addition, in this study, NDVI demonstrated  
376 consistent increases in standard deviation, autocorrelation, and skewness in the unhealthy study  
377 site of Qeshm, indicating significant variations in vegetation density and dynamics (Table. 2).  
378 This behaviour aligns with the expected response of an ecosystem undergoing land cover  
379 changes, providing valuable information about the temporal patterns and health status of the  
380 vegetation. NDVI provided more robust signals compared with MVWR and MNDWI that  
381 exhibited limitations and potential false alarms in assessing ecosystem dynamics. The negative  
382 skewness and negative standard deviation observed in the MVWR index in Qeshm suggest  
383 unreliable signals and interpretations regarding vegetation water content. Similarly, the high

384 autocorrelation and skewness values observed in the MNDWI index raise concerns about its  
385 reliability in detecting water presence. This discrepancy may be attributed to the complex  
386 interaction of various factors in Mangrove Forests such as vegetation health, type, and forest  
387 structure, which have less effects on MNDWI values and lead to inaccurate generation of  
388 warning signals. These findings indicate potential inconsistencies and limitations in using  
389 MNDWI and MDNDWI as standalone indicators for assessing ecosystem health. In contrast,  
390 NDVI's ability to capture changes in vegetation density and its consistent patterns between the  
391 study areas make it a superior indicator. In sum, the varying performance of state variables in  
392 this study can be attributed to the specific characteristics and dynamics of the Mangrove Forest  
393 ecosystem.

394

395 Despite its valuable findings, this study has certain limitations that should be acknowledged.  
396 Firstly, the analysis solely relies on remote sensing data, which may have limitations in  
397 accurately capturing certain ecological processes and dynamics at a finer spatial scale.  
398 Additionally, the study focused on a specific region (Qeshm Island and Gabrik), limiting the  
399 generalizability of the results to other Mangrove Forest ecosystems. However, it should be  
400 noted that, due to the current political situation in some countries such as Iran, accessing field  
401 data is difficult, and thus the common understanding of ecosystem dynamics is strongly based  
402 on satellite data.

## 403 **5. Conclusion**

404

405 This study provides new information on the early warning signals of critical transitions in  
406 Mangrove Forests. By using remote sensing analysis and time series analysis, the capacity to  
407 detect regime shifts in Mangrove Forests globally can be improved. The utilization of remote  
408 sensing indices, particularly NDVI, emerges as a robust indicator of ecosystem dynamics.  
409 NDVI outperforms MVWR and MNDWI in generating early warning signals of critical  
410 transition. This study also highlights notable differences between Mangrove Forest in Qeshm

411 Island and Gabrik study sites, with Qeshm Island showing more pronounced fluctuations and  
412 variability in ecosystem dynamics. The expansion of urban areas on Qeshm Island raises  
413 concerns about potential ecosystem degradation. The practical implications involve informing  
414 policy frameworks and international initiatives for the conservation and sustainable  
415 management of Mangrove Forest ecosystems. The findings contribute to the understanding of  
416 ecosystem dynamics and strengthen the capacity to detect and anticipate critical transitions. To  
417 promote the conservation of Mangrove Forest ecosystems, several policy recommendations  
418 can be made. Strict regulations and land use planning should control urban expansion,  
419 particularly in sensitive coastal regions like Qeshm Island. Buffer zones and protected areas  
420 must be established. Sustainable agricultural practices and reduced use of harmful chemicals  
421 are essential. Raising public awareness through education programs is crucial, along with  
422 fostering collaboration between governmental organizations, research institutions, and local  
423 communities to develop integrated management plans. The findings underscore the need for  
424 region-specific conservation approaches and highlight the value and vulnerability of these  
425 ecosystems. We suggest upscaling the results of this study and developing a generic approach  
426 that provides early warning signals of critical transition in Mangrove Forests on a global scale  
427 to monitor the state of the ecosystem.

428        **6. References**

- 429        Abrantes, K. G., R. Johnston, R. M. Connolly and M. Sheaves (2015). "Importance of  
430 mangrove carbon for aquatic food webs in wet–dry tropical estuaries." Estuaries and Coasts **38**:  
431 383-399.
- 432        Alatorre, L. C., S. Sánchez-Carrillo, S. Miramontes-Beltrán, R. J. Medina, M. E. Torres-Olave,  
433 L. C. Bravo, L. C. Wiebe, A. Granados, D. K. Adams and E. Sánchez (2016). "Temporal  
434 changes of NDVI for qualitative environmental assessment of mangroves: shrimp farming  
435 impact on the health decline of the arid mangroves in the Gulf of California (1990–2010)."  
436 Journal of Arid Environments **125**: 98-109.
- 437        Alibakhshi, S. (2020). Remotely sensed monitoring of land surface albedo and ecosystem  
438 dynamics. Department of Built Environment, Aalto University.
- 439        Alibakhshi, S. (2023). A robust approach and analytical tool for identifying early warning  
440 signals of forest mortality, *Ecological Indicators*. **155**.
- 441        Alibakhshi, S., T. A. Groen, M. Rautiainen and B. Naimi (2017). "Remotely-sensed early  
442 warning signals of a critical transition in a wetland ecosystem." Remote Sensing **9**(4): 352-352.
- 443        Barbier, E. B., E. W. Koch, B. R. Silliman, S. D. Hacker, E. Wolanski, J. Primavera, E. F.  
444 Granek, S. Polasky, S. Aswani and L. A. Cramer (2008). "Coastal ecosystem-based  
445 management with nonlinear ecological functions and values." science **319**(5861): 321-323.
- 446        Bevan, J. M. and M. G. Kendall (1971). "Rank Correlation Methods." The Statistician **20**(3):  
447 74-74.
- 448        Cabello, K., M. Germentil, A. Blanco, E. Macatulad and S. Salmo III (2021). "Post-Disaster  
449 Assessment of Mangrove Forest Recovery in Lawaan-Balangiga, Eastern Samar Using Ndvi  
450 Time Series Analysis." ISPRS Annals of the Photogrammetry, Remote Sensing and Spatial  
451 Information Sciences **3**: 243-250.
- 452        Capon, S. J., A. J. J. Lynch, N. Bond, B. C. Chessman, J. Davis, N. Davidson, M. Finlayson, P.  
453 A. Gell, D. Hohnberg and C. Humphrey (2015). "Regime shifts, thresholds and multiple stable  
454 states in freshwater ecosystems; a critical appraisal of the evidence." Science of the Total  
455 Environment **534**: 122-130.
- 456        Carpenter, S. R. and W. A. Brock (2006). "Rising variance: A leading indicator of ecological  
457 transition." Ecology Letters **9**(3): 311-318.
- 458        Carpenter, S. R. and W. A. Brock (2011). "Early warnings of unknown nonlinear shifts: A  
459 nonparametric approach." Ecology **92**(12): 2196-2201.
- 460        Carpenter, S. R., W. A. Brock, J. J. Cole, J. F. Kitchell and M. L. Pace (2008). "Leading

- 461 indicators of trophic cascades." Ecology Letters **11**(2): 128-138.
- 462 Carpenter, S. R., J. J. Cole, M. L. Pace, R. Batt, W. A. Brock, T. Cline, J. Coloso, J. R. Hodgson,  
463 J. F. Kitchell, D. A. Seekell, L. Smith and B. Weidel (2011). "Early warnings of regime shifts:  
464 A whole-ecosystem experiment." Science **332**(6033): 1079-1082.
- 465 Chen, Y., C. Huang, C. Ticehurst, L. Merrin and P. Thew (2013). "An evaluation of MODIS  
466 daily and 8-day composite products for floodplain and wetland inundation mapping." Wetlands  
467 **33**(5): 823-835.
- 468 Dahdouh-Guebas, F., L. P. Jayatissa, D. Di Nitto, J. O. Bosire, D. L. Seen and N. Koedam  
469 (2005). "How effective were mangroves as a defence against the recent tsunami?" Current  
470 biology **15**(12): R443-R447.
- 471 Dakos, V., S. R. Carpenter, W. A. Brock, A. M. Ellison, V. Guttal, A. R. Ives, S. Kéfi, V. Livina,  
472 D. A. Seekell, E. H. van Nes and M. Scheffer (2012). "Methods for detecting early warnings  
473 of critical transitions in time series illustrated using simulated ecological data." PLoS ONE  
474 **7**(7): e41010-e41010.
- 475 Dakos, V., S. R. Carpenter, E. H. van Nes and M. Scheffer (2015). "Resilience indicators:  
476 Prospects and limitations for early warnings of regime shifts." Philosophical Transactions of  
477 the Royal Society B: Biological Sciences **370**(1659): 1-10.
- 478 Dakos, V., E. H. Van Nes, P. D'Odorico and M. Scheffer (2012). "Robustness of variance and  
479 autocorrelation as indicators of critical slowing down." Ecology **93**(2): 264-271.
- 480 Daru, B. H., K. Yessoufou, L. T. Mankga and T. J. Davies (2013). "A global trend towards the  
481 loss of evolutionarily unique species in mangrove ecosystems." PloS one **8**(6): e66686.
- 482 Duke, N. C., J.-O. Meynecke, S. Dittmann, A. M. Ellison, K. Anger, U. Berger, S. Cannicci, K.  
483 Diele, K. C. Ewel and C. D. Field (2007). "A world without mangroves?" Science **317**(5834):  
484 41-42.
- 485 Ebrahimi-Sirizi, Z. and A. Riyahi-Bakhtiyari (2013). "Petroleum pollution in mangrove forests  
486 sediments from Qeshm Island and Khamir Port—Persian Gulf, Iran." Environmental  
487 monitoring and assessment **185**: 4019-4032.
- 488 Ellison, A. M. (2008). "Managing mangroves with benthic biodiversity in mind: moving  
489 beyond roving banditry." Journal of Sea Research **59**(1-2): 2-15.
- 490 Eslami-Andergoli, L., P. E. R. Dale, J. M. Knight and H. McCallum (2015). Approaching  
491 tipping points: a focussed review of indicators and relevance to managing intertidal ecosystems.  
492 Wetlands Ecology and Management, Kluwer Academic Publishers. **23**: 791-802.
- 493 Giri, C., E. Ochieng, L. Tieszen, Z. Zhu, A. Singh, T. Loveland, J. Masek and N. Duke (2013).  
494 "Global mangrove forests distribution, 2000." NASA Socioeconomic Data and Applications

- 495 [Center \(SEDAC\), Palisades. doi 10: H4J67DW68.](#)
- 496 Giri, C., E. Ochieng, L. L. Tieszen, Z. Zhu, A. Singh, T. Loveland, J. Masek and N. Duke (2011).  
497 "Status and distribution of mangrove forests of the world using earth observation satellite data."  
498 [Global Ecology and Biogeography](#) **20**(1): 154-159.
- 499 Goldberg, L., D. Lagomasino, N. Thomas and T. Fatoyinbo (2020). "Global declines in human-  
500 driven mangrove loss." [Global change biology](#) **26**(10): 5844-5855.
- 501 Gorelick, N., M. Hancher, M. Dixon, S. Ilyushchenko, D. Thau and R. Moore (2017). "Google  
502 Earth Engine: Planetary-scale geospatial analysis for everyone." [Remote Sensing of](#)  
503 [Environment](#) **202**: 18-27.
- 504 Guttal, V. and C. Jayaprakash (2008). "Changing skewness: An early warning signal of regime  
505 shifts in ecosystems." [Ecology Letters](#) **11**(5): 450-460.
- 506 Hirota, M., M. Holmgren, E. H. Van Nes and M. Scheffer (2011). "Global resilience of tropical  
507 forest and savanna to critical transitions." [Science](#) **334**(6053): 232-235.
- 508 Ji, L., L. Zhang and B. Wylie (2009). "Analysis of dynamic thresholds for the normalized  
509 difference water index." [Photogrammetric Engineering and Remote Sensing](#) **75**(11): 1307-  
510 1317.
- 511 Kathiresan, K. (2012). "Importance of mangrove ecosystem." [International Journal of Marine](#)  
512 [Science](#) **2**(10).
- 513 Kéfi, S., V. Guttal, W. A. Brock, S. R. Carpenter, A. M. Ellison, V. N. Livina, D. A. Seekell, M.  
514 Scheffer, E. H. Van Nes and V. Dakos (2014). "Early warning signals of ecological transitions:  
515 Methods for spatial patterns." [PLoS ONE](#) **9**(3): e92097-e92097.
- 516 Kirui, K., J. G. Kairo, J. Bosire, K. M. Viergever, S. Rudra, M. Huxham and R. A. Briers (2013).  
517 "Mapping of mangrove forest land cover change along the Kenya coastline using Landsat  
518 imagery." [Ocean & Coastal Management](#) **83**: 19-24.
- 519 Kourosh Niya, A., J. Huang, H. Karimi, H. Keshtkar and B. Naimi (2019). "Use of intensity  
520 analysis to characterize land use/cover change in the biggest Island of Persian Gulf, Qeshm  
521 Island, Iran." [Sustainability](#) **11**(16): 4396.
- 522 Lenton, T. M. (2011). "Early warning of climate tipping points." [Nature Climate Change](#) **1**(4):  
523 201-209.
- 524 Lenton, T. M., H. Held, E. Kriegler, J. W. Hall, W. Lucht, S. Rahmstorf and H. J. Schellnhuber  
525 (2008). "Tipping elements in the Earth's climate system." [Proceedings of the National Academy](#)  
526 [of Sciences of the United States of America](#) **105**(6): 1786-1793.
- 527 Lenton, T. M., V. N. Livina, V. Dakos, E. H. Van Nes and M. Scheffer (2012). "Early warning

- 528 of climate tipping points from critical slowing down: Comparing methods to improve  
529 robustness." Philosophical Transactions of the Royal Society A: Mathematical, Physical and  
530 Engineering Sciences **370**(1962): 1185-1204.
- 531 Li, H., M. Jia, R. Zhang, Y. Ren and X. Wen (2019). "Incorporating the plant phenological  
532 trajectory into mangrove species mapping with dense time series Sentinel-2 imagery and the  
533 Google Earth Engine platform." Remote Sensing **11**(21): 2479.
- 534 Li, W., Q. Chen, D. Cai and R. Li (2015). "Determination of an appropriate ecological  
535 hydrograph for a rare fish species using an improved fish habitat suitability model introducing  
536 landscape ecology index." Ecological Modelling **311**: 31-38.
- 537 Lugendo, B. R., I. Nagelkerken, G. Kruitwagen, G. Van Der Velde and Y. D. Mgaya (2007).  
538 "Relative importance of mangroves as feeding habitats for fishes: a comparison between  
539 mangrove habitats with different settings." Bulletin of Marine Science **80**(3): 497-512.
- 540 Luther, D. A. and R. Greenberg (2009). "Mangroves: a global perspective on the evolution and  
541 conservation of their terrestrial vertebrates." BioScience **59**(7): 602-612.
- 542 Martínez, M. L., A. Intralawan, G. Vázquez, O. Pérez-Maqueo, P. Sutton and R. Landgrave  
543 (2007). "The coasts of our world: Ecological, economic and social importance." Ecological  
544 economics **63**(2-3): 254-272.
- 545 Mazraeh, H. M. and M. Pazhouhanfar (2018). "Effects of vernacular architecture structure on  
546 urban sustainability case study: Qeshm Island, Iran." Frontiers of architectural research **7**(1):  
547 11-24.
- 548 Mozumder, C., N. K. Tripathi and T. Tipdecho (2014). "Ecosystem evaluation (1989–2012) of  
549 Ramsar wetland Deepor Beel using satellite-derived indices." Environmental Monitoring and  
550 Assessment **186**(11): 7909-7927.
- 551 Muñoz Sabater, J. (2019). "ERA5-land monthly averaged data from 1981 to present,  
552 Copernicus Climate Change Service (C3S) Climate Data Store (CDS)." Earth Syst. Sci. Data  
553 **55**: 5679-5695.
- 554 Naderloo, R., M. Türkay and A. Sari (2013). "Intertidal habitats and decapod (Crustacea)  
555 diversity of Qeshm Island, a biodiversity hotspot within the Persian Gulf." Marine biodiversity  
556 **43**: 445-462.
- 557 Nagelkerken, I., G. Van der Velde, M. Gorissen, G. Meijer, T. Van't Hof and C. Den Hartog  
558 (2000). "Importance of mangroves, seagrass beds and the shallow coral reef as a nursery for  
559 important coral reef fishes, using a visual census technique." Estuarine, coastal and shelf  
560 science **51**(1): 31-44.
- 561 Pinheiro, J., D. Bates, S. DebRoy and D. Sarkar (2000). "the R Development Core Team, 2013."

- 562 NLME: linear and nonlinear mixed effects models: 1-3.
- 563 Polidoro, B. A., K. E. Carpenter, L. Collins, N. C. Duke, A. M. Ellison, J. C. Ellison, E. J.  
564 Farnsworth, E. S. Fernando, K. Kathiresan and N. E. Koedam (2010). "The loss of species:  
565 mangrove extinction risk and geographic areas of global concern." PloS one **5**(4): e10095.
- 566 Qgis, S. (2016). QGIS Geographic Information System v.2.16.3. Open Source Geospatial  
567 Foundation. URL: <http://qgis.osgeo.org>.
- 568 Rokni, K., A. Ahmad, A. Selamat and S. Hazini (2014). "Water feature extraction and change  
569 detection using multitemporal landsat imagery." Remote Sensing **6**(5): 4173-4189.
- 570 Ruan, L., M. Yan, L. Zhang, X. Fan and H. Yang (2022). "Spatial-temporal NDVI pattern of  
571 global mangroves: A growing trend during 2000–2018." Science of The Total Environment **844**:  
572 157075.
- 573 Scheffer, M. (1990). Multiplicity of stable states in freshwater systems. Hydrobiologia,  
574 Springer. **200-201**: 475-486.
- 575 Scheffer, M. (2001). "Alternative attractors of shallow lakes." TheScientificWorldJournal **1**:  
576 254-263.
- 577 Scheffer, M., J. Bascompte, W. A. Brock, V. Brovkin, S. R. Carpenter, V. Dakos, H. Held, E.  
578 H. Van Nes, M. Rietkerk and G. Sugihara (2009). "Early-warning signals for critical  
579 transitions." Nature **461**(7260): 53-59.
- 580 Scheffer, M., S. Carpenter, J. A. Foley, C. Folke and B. Walker (2001). "Catastrophic shifts in  
581 ecosystems." Nature **413**(6856): 591-596.
- 582 Shimu, S. A., M. Aktar, M. I. Afjal, A. M. Nitu, M. P. Uddin and M. Al Mamun (2019). NDVI  
583 based change detection in Sundarban Mangrove Forest using remote sensing data. 2019 4th  
584 International Conference on Electrical Information and Communication Technology (EICT),  
585 IEEE.
- 586 Sorichetta, A., G. M. Hornby, F. R. Stevens, A. E. Gaughan, C. Linard and A. J. Tatem (2015).  
587 "High-resolution gridded population datasets for Latin America and the Caribbean in 2010,  
588 2015, and 2020." Scientific data **2**(1): 1-12.
- 589 Tajbakhsh, A., A. Karimi and A. Zhang (2020). "Modeling land cover change dynamic using a  
590 hybrid model approach in Qeshm Island, Southern Iran." Environmental monitoring and  
591 assessment **192**: 1-17.
- 592 Tehrani, N. A. and M. Janalipour (2021). "Predicting ecosystem shift in a Salt Lake by using  
593 remote sensing indicators and spatial statistics methods (case study: Lake Urmia basin)."  
594 Environmental Engineering Research **26**(4).

595 Toosi, N. B., A. R. Soffianian, S. Fakheran, S. Pourmanafi, C. Ginzler and L. T. Waser (2019).  
596 "Comparing different classification algorithms for monitoring mangrove cover changes in  
597 southern Iran." Global Ecology and Conservation **19**: e00662.

598 Tran, T. V., R. Reef and X. Zhu (2022). "A Review of Spectral Indices for Mangrove Remote  
599 Sensing." Remote Sensing **14**(19): 4868.

600 Verbesselt, J., R. Hyndman, G. Newnham and D. Culvenor (2010). "Detecting trend and  
601 seasonal changes in satellite image time series." Remote Sensing of Environment **114**(1): 106-  
602 115.

603 Verbesselt, J., R. Hyndman, A. Zeileis and D. Culvenor (2010). "Phenological change detection  
604 while accounting for abrupt and gradual trends in satellite image time series." Remote Sensing  
605 of Environment **114**(12): 2970-2980.

606 Verbesselt, J., N. Umlauf, M. Hirota, M. Holmgren, E. H. Van Nes, M. Herold, A. Zeileis and  
607 M. Scheffer (2016). "Remotely sensed resilience of tropical forests." Nature Climate Change  
608 **6**(11): 1028-1031.

609 Wang, F., J. Zhang, Y. Cao, R. Wang, G. Kattel, D. He and W. You (2023). "Pattern changes  
610 and early risk warning of *Spartina alterniflora* invasion: a study of mangrove-dominated  
611 wetlands in northeastern Fujian, China." Journal of Forestry Research: 1-16.

612 Xu, H. (2006). "Modification of normalised difference water index (NDWI) to enhance open  
613 water features in remotely sensed imagery." International Journal of Remote Sensing **27**(14):  
614 3025-3033.

615 Yessoufou, K. and G. Stoffberg (2016). "Biogeography, threats and phylogenetic structure of  
616 mangrove forest globally and in South Africa: A review." South African Journal of Botany **107**:  
617 114-120.

618 Zahed, M. A., F. Rouhani, S. Mohajeri, F. Bateni and L. Mohajeri (2010). "An overview of  
619 Iranian mangrove ecosystems, northern part of the Persian Gulf and Oman Sea." Acta  
620 Ecologica Sinica **30**(4): 240-244.

621